General Choice of the Regularization Functional in Regularized Image Restoration

Moon Gi Kang and Aggelos K. Katsaggelos, *Senior Member, IEEE*

Abstract— **The determination of the regularization parameter is an important issue in regularized image restoration, since it controls the trade-off between fidelity to the data and smoothness of the solution. A number of approaches have been developed in determining this parameter. In this paper, a new paradigm is adopted, according to which the required prior information is extracted from the available data at the previous iteration step, i.e., the partially restored image at each step. We propose the use of a regularization functional instead of a constant regularization parameter. The properties such a regularization functional should satisfy are investigated, and two specific forms of it are proposed. An iterative algorithm is proposed for obtaining a restored image. The regularization functional is defined in terms of the restored image at each iteration step, therefore allowing for the simultaneous determination of its value and the restoration of the degraded image. Both proposed iteration adaptive regularization functionals are shown to result in a smoothing functional with a global minimum, so that its iterative optimization does not depend on the initial conditions. The convergence of the algorithm is established and experimental results are shown.**

I. Introduction

IMAGE restoration has been extensively studied and used in several areas of science and engineering [1]–[3]. For example, stellar images observed by ground-base telescopes are degraded due to atmospheric turbulence, while there are also applications where the stellar images need to be restored even if they are not observed through the atmosphere. A prime example is images obtained by the Hubble Space Telescope [4], which are seriously degraded due to the spherical aberration of its primary mirror. As another example, the study of motion blur becomes important when longer exposures are necessary to record relatively dark scenes or when, for example, the image motion-compensation system on a satellite fails.

In most cases, the image degradation process can be modeled by a linear blur and an additive white Gaussian noise process [1], that is

$$y = Dx + n \tag{1}$$

where the vectors y, x and n represent, respectively, the lexicographically ordered noisy blurred image, the deterministic original image, and the additive noise. The matrix D represents the linear distortion, which may be space-invariant or variant. The image restoration problem calls for applying an inverse procedure to obtain an approximation of the original image x based on the image degradation model. It is an ill-posed problem, which means that a small perturbation in the data leads to a large perturbation in the solution. Therefore, a solution should be estimated balancing fidelity to the data and smoothness of the solution, which represents the basic idea of regularization [5].

Based on the image degradation model of (1), there have been a number of approaches developed to restore the original image x, given the observed image y, D and some knowledge about the noise n (for a recent review and classification of the various restoration approaches, see [3], chapter 1). Among these is the set theoretic approach presented in [6], [7], which has Miller's regularization approach [8] and the constrained least-squares (CLS) approach [9] as special cases. According to this approach, a quadratic smoothing functional is defined that combines fidelity to the data with prior knowledge. An expression of it is given by

$$M(\alpha, x) = \|y - Dx\|^2 + \alpha\|Cx\|^2 \tag{2}$$

where C is a linear highpass operator and α is the regularization parameter controlling the contribution of the terms $\|y - Dx\|^2$ and $\|Cx\|^2$. The restored image is the vector $\hat{x}$, which minimizes the functional $M(\alpha, x)$.

If bounds of $\|y - Dx\|^2$ and $\|Cx\|^2$, denoted respectively by ϵ^2 and E^2, are known, then α is given as $(\epsilon/E)^2$ [6]–[8]. If only one of the bounds is known, a CLS approach can be followed [9]. According to the CLS approach, the restoration problem is solved based on an initial estimate of α, α is then adjusted based on the restored image, and the process is repeated until either $\|y - Dx\|^2 = \epsilon^2$ or $\|Cx\|^2 = E^2$, depending on which of the bounds is known. Other approaches for determining the regularization parameter without requiring knowledge of ϵ^2 of E^2 are based on the methods of cross-validation [10]–[12] and maximum likelihood [12]. All of these methods, however, determine the regularization parameter in a separate first step, resulting in additional computational overhead.

In our previous work [13]–[15], we proposed iteration adaptive restoration algorithms, according to which both bounds E and ϵ are updated at each iteration step based on the available restored image. Although the algorithms provide an efficient way to simultaneously determine the regularization parameter and restore the image without any prior knowledge about the

Manuscript received August 18, 1993; revised April 5, 1994. This work was supported by a grant from the Space Telescope Science Institute, Baltimore, MD. The associate editor coordinating the review of this paper and approving it for publication was Prof. Xinhua Zhuang.

M. G. Kang is with the Department of Elelctrical and Computer Engineering, University of Minnesota, Duluth, MN 55812 USA.

A. K. Katsaggelos is with the Department of Electrical Engineering and Computer Science, McCormick School of Engineering and Applied Science, Northwestern University, Evanston, IL 60208-3118 USA.

IEEE Log Number 9410201.

bounds, the functional to be minimized has more than one local minimizer, so that the iteration depends on the initial conditions.

In this paper, we propose an iteration adaptive algorithm that also simultaneously determines the regularization parameter based on the restored image at each step and restores the image. This algorithm, however, does not depend on the initial conditions, or, in other words, the smoothing functional to be minimized is shown to have a unique minimizer. An accurate estimate of the noise variance is obtained at convergence. The approach we propose in this paper presents a paradigm according to which properties of the original image are extracted from the partially restored image at each iteration step. In turn, such properties are used to guide the restoration. Although the partially restored image is only used to define the value of the regularization parameter, other uses of it may potentially be developed.

The paper is organized as follows. In Section II, a regularization functional is introduced, to be used in the place of a constant regularization parameter. The desired properties of this and the smoothing functionals are analyzed, and the convexity of the latter is shown. Two forms of the regularization functional are proposed and analyzed. In Section III, an iterative algorithm is proposed to obtain the minimum of the smoothing functional. The algorithm is analyzed, and a sufficient condition for its convergence is established. Experimental results are presented in Section IV, and conclusions are reached in Section V.

II. General Choice of the Regularization Parameter

The main objective in our work is to employ an iterative algorithm to estimate the regularization parameter at the same time with the restored image. The available estimate of the restored image at each iteration step will be used for determining the value of the regularization parameter. That is, the regularization parameter is defined as a function of the original image (and eventually in practice of an estimate of it). Of great importance is the form of this functional, so that the smoothing functional to be minimized preserves its convexity and exhibits only a global minimizer. We therefore propose the use of

$$M(\alpha(x), x) = \|y - Dx\|^2 + \alpha(x)\|Cx\|^2 \tag{3}$$

as the functional to be minimized. $\alpha(x)$ maps a vector x onto the positive real line. Its purpose is, as before, to control the relative contribution of the error term $\|y - Dx\|^2$, which enforces "faithfulness" to the data, and the stabilizing functional $\|Cx\|^2$, which enforces smoothness on the solution. Its dependency, however, on the original image, as well as the available data, is explicitly utilized. This dependency, on the other hand, is implicitly utilized in the CLS approach, according to which the minimization of $M(\alpha, x)$ in (2) and the determination of the regularization parameter α are completely separate steps. In the following, the required properties of $\alpha(x)$ and $M(\alpha(x), x)$, which will make the minimization of $M(\alpha(x), x)$ meaningful, are presented and analyzed.

A. Properties of the Regularization and Smoothing Functionals

Various choices of the functional $\alpha(x)$ can potentially result in meaningful minimizers of $M(\alpha(x), x)$ in (3). The following three properties of $\alpha(x)$ and $M(\alpha(x), x)$ are considered necessary for such an objective [16].

Property 1: $\alpha(x)$ should be a function of the smoothing functional: We choose $\alpha(x)$ to be proportional to $M(\alpha(x), x)$, which represents the regularized noise power. That is, we set in general

$$\alpha(x) = f(M(\alpha(x), x)) \tag{4}$$

where $f(\cdot)$ is a monotonically increasing function. The justification behind this choice of $\alpha(x)$ is based on the set theoretic formulation of the restoration problem [6], [7], [17]. According to it, $\alpha(x)$ is proportional to $\|y - Dx\|^2$, that is

$$\alpha(x) \sim \|y - Dx\|^2. \tag{5}$$

It should also be inversely proportional to the low-frequency energy of the restored image, according to

$$\alpha(x) \sim \left(1 - \frac{\|Cx\|^2}{\|x\|^2}\right)^{-1}. \tag{6}$$

In other words, if the energy of a restoration at low frequencies is relatively large (meaning that the energy at high frequencies is small, under the assumption of constant total energy), then a smaller value of $\alpha(x)$ should be used, so that the higher frequencies are further restored. The opposite should occur if the energy of a restoration at low frequencies is relatively small. This property (6) can be rewritten as

$$\alpha(x) \sim \alpha(x)\|Cx\|^2. \tag{7}$$

Properties (5) and (7) result in (4).

A consequence of the choice of $\alpha(x)$ in (4) is that an optimal estimate $\hat{x}$, which satisfies $\nabla_x M(\alpha(\hat{x}), \hat{x}) = 0$, also satisfies $\nabla_x \alpha(\hat{x}) = 0$. This is the case since

$$\nabla_x \alpha(x) = \nabla_x f(M) = \frac{df(M)}{dM} \nabla_x M(\alpha(x), x) \tag{8}$$

provided $\frac{df(M)}{dM}$ is finite. This last observation will prove useful in obtaining a suitable expression for the restored image and for analyzing the convergence of the iterative algorithm that will be employed, as will be shown in the next section.

Property 2: Extreme minimizers of $M(\alpha(x), x)$: Another desired property of $M(\alpha(x), x)$ is that its minimizer should represent a solution between two extreme solutions: one representing the generalized inverse solution of (1), when the data are noiseless, and the other representing the smoothest possible solution ($x = 0$), when the noise power becomes infinite. These requirements translate into the conditions

$$\alpha(x) = f(M(\alpha(x), x)) = 0, \text{ when } \|n\|^2 = \|y - Dx\|^2 = 0 \tag{9}$$

and

$$\alpha(x) = f(M(\alpha(x), x)) = \infty \quad \text{when } \|n\|^2 = \|y - Dx\|^2 = \infty. \tag{10}$$

Conditions (9) and (10) result in

$$f(M(\alpha(x),x)) = 0, \text{ when } M(\alpha(x),x) = 0 \quad (11)$$

and

$$f(M(\alpha(x),x)) = \infty, \text{ when } M(\alpha(x),x) = \infty. \quad (12)$$

Therefore, $f(M)$ and consequently $\alpha(x)$ should map (0, ∞) into (0, ∞) and be a monotonically increasing function of M.

Property 3: The functional $M(\alpha(x),x)$ should be convex for all choices of $\alpha(x)$: This requirement on convexity is obviously very important, since a local extremum of a nonlinear functional becomes a global extremum, if the functional is convex. Therefore, the iterative algorithm that will be employed for obtaining a minimizer of $M(\alpha(x),x)$ will not depend on the initial condition. Clearly, for $\alpha(x) = c$, a constant independent of x, $M(\alpha(x),x)$ is convex. In our previous work [13], [14], nonlinear functionals for $\alpha(x)$ were used that did not preserve the convexity of $M(\alpha(x),x)$.

In the following, conditions on $\alpha(x)$ are derived for preserving the convexity of $M(\alpha(x),x)$. Furthermore, two specific functions $f(M)$ are proposed that satisfy all three properties outlined above.

B. Convexity of $M(\alpha(x),x)$

A real valued functional h defined on a convex subset C of a linear vector space is said to be convex if

$$h(az_1 + (1-a)z_2) \le ah(z_1) + (1-a)h(z_2) \quad (13)$$

for all $z_1, z_2 \in C$ and $0 < a < 1$. If strict inequality holds whenever $z_1 \neq z_2$, h is said to be strictly convex. h is defined as concave if $-h$ is convex [18].

Let us rewrite the nonlinear functional $M(\alpha(x),x)$ of (3) with the use of (4) as

$$M(z) = M(p,q) = p + f(M(p,q))q \quad (14)$$

where z is a 2-D vector, with elements $p = \|y - Dx\|^2$ and $q = \|Cx\|^2$. p and q are defined within a convex region, i.e., $p, q \in C$. The condition for convexity of the nonlinear functional $M(\alpha(x),x)$ translates into the condition

$$M(az_1 + (1-a)z_2) \le aM(z_1) + (1-a)M(z_2) \quad (15)$$

or

$$M(ap_1 + (1-a)p_2, aq_1 + (1-a)q_2) \le aM(p_1,q_1) + (1-a)M(p_2,q_2) \quad (16)$$

where the two vectors z_1 and z_2 are defined as $z_1 = (p_1,q_1)^T$ and $z_2 = (p_2,q_2)^T$, respectively, $p_1, q_1, p_2, q_2 \in C$ and $0 < a < 1$. As shown in Appendix A, if $f(M)$ is a linear function of M and the condition

$$\frac{\partial f(M)}{\partial M} < \frac{1}{\|Cx\|^2} \quad (17)$$

is satisfied, $M(\alpha(x),x)$ is convex. If $f(M)$ is a nonlinear function of M, although no rigorous proof has been found, the convexity of $M(\alpha(x),x)$ has been verified experimentally.

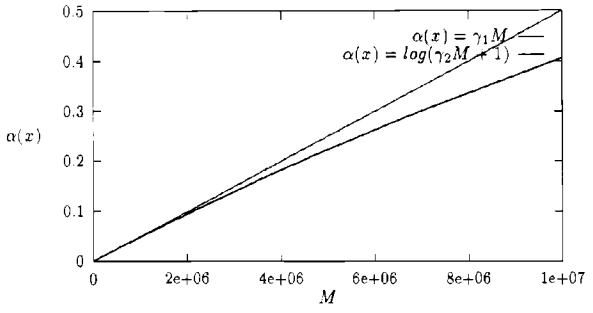

Fig. 1. Comparison of $\gamma_1 M(\alpha(x),x)$ and $\ln(\gamma_2 M(\alpha(x),x)+1)$ for values of γ_1 and γ_2 resulting, respectively, from the convexity and convergence analyses.

C. Proposed Forms of the Regularization Functional

We have investigated three desirable properties of the regularization functional. We now propose certain functionals that have these properties. The first one is a linear function of the form

$$\alpha(x) = f(M) = \gamma_1 M(\alpha(x),x) \quad (18)$$

where γ_1 is the coefficient representing the slope of the line and also controls convexity. It is straightforward to show that this function satisfies all three properties. Equation (18) can be rewritten as

$$\alpha(x) = \frac{\|y - Dx\|^2}{(1/\gamma_1) - \|Cx\|^2}. \quad (19)$$

In order for this choice of $\alpha(x)$ to satisfy Property 3, the control parameter γ_1 should be less than $(1/\|Cx\|^2)$, since $\frac{\partial f(M)}{\partial M} = \gamma_1$.

The second functional proposed is of the form

$$\alpha(x) = f(M) = \ln(\gamma_2 M + 1) \quad (20)$$

which also satisfies Properties 1 and 2. As already mentioned above, the proof of convexity of $M(\alpha(x),x)$ presented in Appendix A does not apply to this form of the functional due to its nonlinearity. It is still useful, however, since, as is experimentally shown, $M(\alpha(x),x)$ has a unique minimum. Additionally, the range of values of γ_2 that is specified by the convergence analysis to be presented in the next section is such that the $\ln(\gamma_2 M + 1)$ function is almost linear for the usable range of values of M. An example is shown in Fig. 1, where $\gamma_1 M$ and $\ln(\gamma_2 M + 1)$ are compared for values of γ_1 and γ_2 resulting, respectively, from the convexity and convergence analyses.

We can also consider approximations to the expression for $\alpha(x)$ in (20) for any values of γ_2 and M. From (20), we have

$$e^{\alpha(x)} = \gamma_2 M(\alpha(x),x) + 1. \quad (21)$$

Using Taylor series expansion, we further obtain

$$e^{\alpha(x)} = 1 + \alpha(x) + R(0^2) = 1 + \alpha(x) + \frac{\alpha^2(x)}{2} + R(0^3). \quad (22)$$

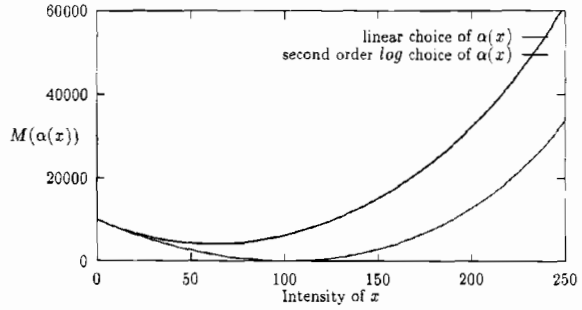

Fig. 2. $M(\alpha(x), x)$ versus x (scalar) for two choices of $\alpha(x)$.

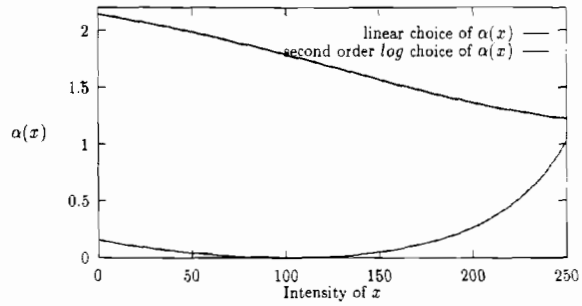

Fig. 3. Two choices of $\alpha(x)$ versus x (scalar).

If $\alpha(x)$ is small enough to ignore $R(0^2)$, then $e^{\alpha(x)}$ is approximated to be linear and

$$1 + \alpha(x) = \gamma_2 M(\alpha(x), x) + 1$$

or

$$\alpha(x) = \frac{\|y - Dx\|^2}{(1/\gamma_2) - \|Cx\|^2} \tag{23}$$

which is the same expression with that in (19). If we consider the second-order term and ignore $R(0^3)$, then

$$1 + \alpha(x) + \frac{\alpha^2(x)}{2} = \gamma_2 M(\alpha(x), x) + 1$$

or

$$\alpha(x) = \gamma_2\|Cx\|^2 - 1 + \sqrt{(1 - \gamma_2\|Cx\|^2)^2 + 2\gamma_2\|y - Dx\|^2}. \tag{24}$$

Fig. 2 shows the form of the smoothing functional $M(\alpha(x), x)$ as a function of a scalar x for the choices of $\alpha(x)$ in (23) and (24). It is clear that in both cases $M(\alpha(x), x)$ is convex. Fig. 3 shows a plot of $\alpha(x)$ in (23) and (24) for a scalar x, which were used for generating $M(\alpha(x), x)$ of Fig. 2. The values of γ_1 and γ_2 in both figures are determined from the convexity and convergence analyses.

As shown in Fig. 1, this latter choice of the regularization functional is emphasizing the larger regularized noise power less than the first linear choice, which means that this choice emphasizes more fidelity to the data.

III. An Iterative Restoration Algorithm

As has already been mentioned, a restored image is a minimizer of the smoothing functional $M(\alpha(x), x)$ defined in (3). Since it was shown that $M(\alpha(x), x)$ is convex, for choices of $\alpha(x)$ that satisfy certain properties, if there exists a minimizer it will be a unique and therefore global minimizer. We show that there exists a minimizer of $M(\alpha(x), x)$ by establishing sufficient conditions for an iteration to converge to a vector satisfying the necessary conditions for an optimum of $M(\alpha(x), x)$. The necessary condition for a minimum is that the gradient of $M(\alpha(x), x)$ with respect to x is equal to zero, that is

$$\nabla_x M(\alpha(x), x) = 2(D^T D + \alpha(x) C^T C)x + \|Cx\|^2 \nabla_x \alpha(x) - 2D^T y = 0. \tag{25}$$

Since $\nabla_x \alpha(x) = 0$, the equation for the optimal solution becomes

$$(D^T D + \alpha(x) C^T C)x = D^T y. \tag{26}$$

Since (26) is nonlinear, it is solved by employing the successive approximations iteration

$$x_{k+1} = x_k + [D^T y - (D^T D + \alpha(x_k) C^T C)x_k]. \tag{27}$$

It is mentioned here that no relaxation parameter is used in the above iteration, since another control parameter (γ_1 or γ_2), which is used for defining $\alpha(x)$, is also used for defining the convergence of the algorithm. Iteration (25) can be initialized with any vector since $M(\alpha(x), x)$ has a global minimizer.

A. Convergence Analysis

Rewriting iteration (27) for two consecutive values of k, we obtain

$$x_{k+1} - x_k = (x_k - x_{k-1}) - D^T D(x_k - x_{k-1}) - C^T C(F(x_k) - F(x_{k-1})) \tag{28}$$

where the nonlinear factor is equal to $F(x_k) = \alpha(x_k)x_k$. This factor is linearized using the Jacobian matrix, and (28) is rewritten as

$$x_{k+1} - x_k = [I - (D^T D + C^T C J_F(x_k))](x_k - x_{k-1}). \tag{29}$$

The mnth element of the Jacobian matrix $J_F(x)$ is equal to

$$\frac{\partial F_m(x)}{\partial x_n} = x_m \frac{\partial \alpha(x)}{\partial x_m} + \alpha(x) \frac{\partial x_m}{\partial x_n} \tag{30}$$

where $F_m(x)$ is the mth element of the nonlinear vector F and x_n denotes the nth element of the vector x. Since $\nabla_x \alpha(x) = 0$ when $\nabla_x M(\alpha(x), x) = 0$, the Jacobian matrix becomes a diagonal matrix whose diagonal element is $\alpha(x)$, that is

$$J_F(x) = \alpha(x) I. \tag{31}$$

If we consider the norm of both sides of (29), we obtain

$$\|x_{k+1} - x_k\| \le \|I - (D^T D + \alpha(x_k) C^T C)\| \cdot \|x_k - x_{k-1}\|. \tag{32}$$

According to (32), the condition

$$\|I - (D^T D + \alpha(x_k) C^T C)\| < 1 \tag{33}$$

is sufficient for convergence of the iteration. Since $(D^T D + \alpha(x_k) C^T C)$ is a positive definite matrix (C is chosen appropriately to guarantee this), this condition is rewritten with the use of l_2 matrix norms as

$$|1 - \sigma_{\max}(D^T D + \alpha(x_k) C^T C)| < 1$$

and thus

$$0 \leq \sigma_{\max}(D^T D + \alpha(x_k) C^T C) < 2 \tag{34}$$

where $\sigma_{\max}(Q)$ denotes the maximum singular value of the matrix Q. Using the triangular inequality, we have

$$\sigma_{\max}(D^T D + \alpha(x_k) C^T C) \leq \sigma_{\max}(D^T D) + \alpha(x_k)\sigma_{\max}(C^T C) \tag{35}$$

or

$$\sigma_{\max}(D^T D) + \alpha(x_k)\sigma_{\max}(C^T C) < 2. \tag{36}$$

Therefore, the sufficient condition for convergence becomes

$$\alpha(x_k) < \frac{2 - \sigma_{\max}(D^T D)}{\sigma_{\max}(C^T C)} = 1 \tag{37}$$

since matrices D and C are normalized, that is $\sigma_{\max}(D^T D) = \sigma_{\max}(C^T C) = 1$.

B. Choices of the Control Parameters γ_1 and γ_2

The sufficient condition for convergence (37) is used next in determining the appropriate values of the control parameters γ_1 and γ_2, which were introduced in the previous section. We assume that the restored image at every iteration step is bounded.

1) Linear Regularization Functional: Condition (37) in this case takes the form

$$\alpha(x_k) = \frac{\|y - Dx_k\|^2}{(1/\gamma_1) - \|Cx_k\|^2} < 1$$

and thus

$$\frac{1}{\gamma_1} \geq \|Cx_k\|^2 + \|y - Dx_k\|^2. \tag{38}$$

Since

$$\|Cx_k\|^2 \leq \|C\|^2 \|x_k\|^2 = \|x_k\|^2 \simeq \|y\|^2 \tag{39}$$

and

$$\|y - Dx\|^2 = \|n\|^2 \leq \|y\|^2 = \|Dx + n\|^2 \tag{40}$$

(the latter is true since all elements of Dx are positive), (38) results in

$$\frac{1}{\gamma_1} \geq 2\|y\|^2. \tag{41}$$

If we use equality in (41), then the condition for convexity (17) is also satisfied, that is

$$\frac{\partial \alpha(x)}{\partial M} = \gamma_1 = \frac{1}{2\|y\|^2} \leq \frac{1}{\|Cx\|^2}. \tag{42}$$

TABLE I
CONVERGED REGULARIZATION PARAMETERS OF THE PROPOSED ALGORITHMS: α_L: LINEAR; α_Q: QUADRATIC; α_{ST}: SET THEORETIC

SNR	20dB				30dB			
x_0	$D^T y$	$C^T y$	$CD^T y$	10^9	$D^T y$	$C^T y$	$CD^T y$	10^9
$\alpha_L(x)$	0.084	0.084	0.084	0.084	0.0090	0.0090	0.0090	0.0090
$\alpha_Q(x)$	0.080	0.080	0.080	0.080	0.0090	0.0090	0.0090	0.0090
$\alpha_{ST}(x)$	0.091	7×10^{-4}	4×10^{-3}	0.091	0.011	6×10^{-5}	5×10^{-4}	0.0010

2) Quadratic Regularization Functional: Condition (37) in this case takes the form

$$\gamma_2\|Cx\|^2 - 1 + \sqrt{(1 - \gamma_2\|Cx\|^2)^2 + 2\gamma_2\|y - Dx\|^2} \leq 1. \tag{43}$$

From it, it is straightforward to get the condition

$$\gamma_2 \leq \frac{3}{2\|Cx_k\|^2 + 2\|y - Dx\|^2}. \tag{44}$$

Therefore, with the use of (39) and (40), we obtain

$$\frac{1}{\gamma_2} \geq \frac{4}{3}\|y\|^2. \tag{45}$$

This choice also satisfies the condition for convexity (17), assuming that the linear part of the ln function is considered, since

$$\frac{\partial \alpha(x)}{\partial M} = \frac{1}{M(\alpha(x), x) + (1/\gamma_2)} = \frac{1}{M(\alpha(x), x) + \frac{4}{3}\|y\|^2} \leq \frac{1}{\|Cx_k\|^2}. \tag{46}$$

IV. EXPERIMENTAL RESULTS

The performance of the proposed iteration adaptive image restoration algorithm with the two choices of the regularization functional is studied experimentally. In these experiments, a 256×256 pixels portrait image is used, the degradation D is due to a 7×7 uniform blur, the 2-D Laplacian is used for C, and the criterion $\|x_{k+1} - x_k\|^2/\|x_k\|^2 \leq 10^{-6}$ is used for terminating the iteration. As mentioned in the previous section, the control parameters, γ_1 and γ_2, are chosen according to

$$\frac{1}{\gamma_1} = 2\|y\|^2 \text{ and } \frac{1}{\gamma_2} = \frac{4}{3}\|y\|^2. \tag{47}$$

The performance of the restoration algorithm is evaluated by measuring the improvement in signal to noise ratio after k-iterations denoted by Δ^k_{SNR} and defined by

$$\Delta^k_{\text{SNR}} = 10\log_{10}\frac{\|y - x\|^2}{\|x_k - x\|^2}. \tag{48}$$

These algorithms were run with various initial values of x_0 to demonstrate that the values of $\alpha(x)$ and the final solution are independent of the initial conditions and that convergence to a unique minimizer is obtained. They are also compared with the iteration adaptive algorithm in [14] that depends on the initial condition. A lowpass filtered version of the observed image $D^T y$, the observed image y, a highpass filtered version of the observed image $C^T y$, and a bandpass filtered version of the observed image $CD^T y$ are used for the initial input image x_0. The values of the regularization functionals proposed in this paper and in [14] are shown in Table I. A large

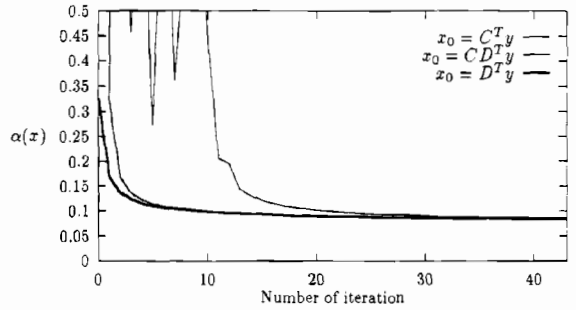

Fig. 4. Linear $\alpha(x)$ versus iteration number of various initial conditions (SNR = 20 dB).

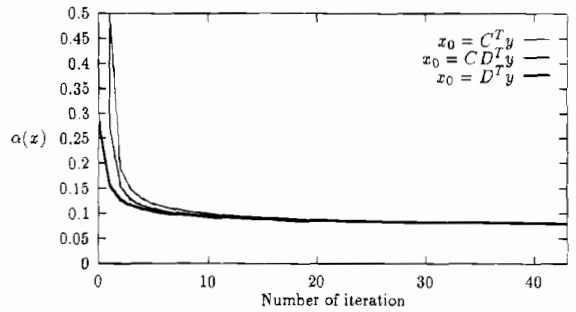

Fig. 5. Quadratic $\alpha(x)$ versus iteration number of various initial conditions (SNR = 20 dB).

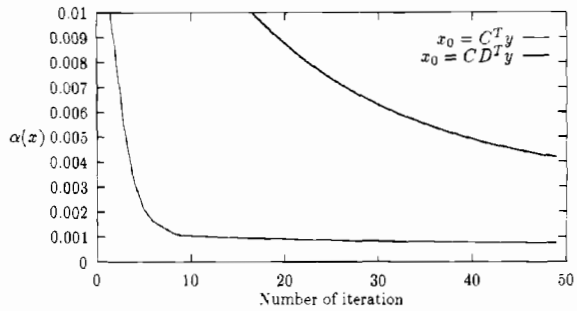

Fig. 6. $\alpha(x)$ in [14] versus iteration number of various initial conditions (SNR = 20 dB).

constant value, $x_0 = 10^9$, is also used as initial condition in testing experimentally the assumption on the boundedness of x_k. In Figs. 4 and 5, both of the proposed iteration adaptive regularization functionals are shown to converge to the same value independently of the initial conditions. In Fig. 6, the regularization functional proposed in [14] based on a set theoretic regularization approach is shown versus the iteration number for two different initial conditions. Unlike the curves in Figs. 4 and 5, $\alpha(x)$ converges to two different values that are both quite small, resulting in a noisy restored image close to the inverse solution.

In Figs. 7 and 8, the two quadratic terms in the functional $M(\alpha(x), x)$ normalized by the number of pixels N, i.e., the residual term $\|y - Dx_k\|^2/N^2$ (the two curves are indistinguishable) and the highpass image energy term $\|Cx_k\|^2/N^2$

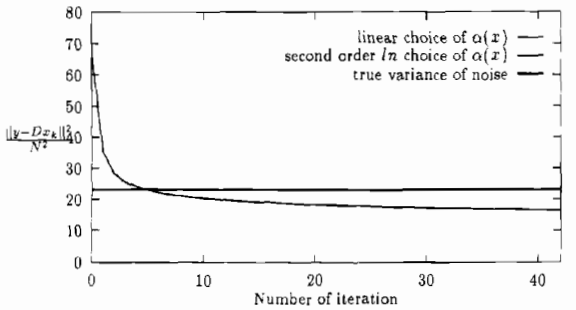

Fig. 7. Values of $\|y-D_{x_k}\|^2/N^2$ versus iteration number (SNR = 20 dB).

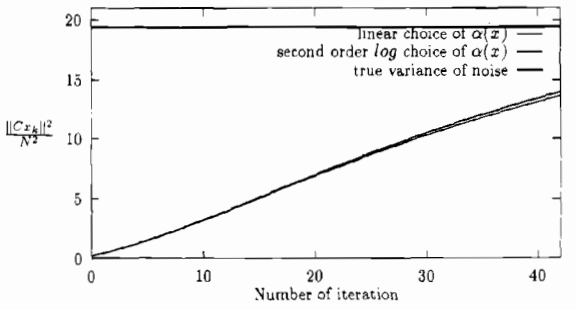

Fig. 8. Values of $\|C_{x_k}\|^2/N^2$ versus iteration number (SNR = 20 dB).

are shown. The values of these terms at convergence are slightly smaller than the values based on the original image, which is available in a simulation. That is, as a by-product of the algorithm, an accurate estimate of the variance of the additive noise is obtained. By examining steps $\|x_k - x_{k-1}\|^2$, it is observed that the proposed algorithms converge with the same rate. The noisy blurred images are shown in Figs. 9(a) (SNR = 20 dB) and 10(b) (SNR = 30 dB). The corresponding restored images of Fig. 9(a) by the two choices of the regularization functional are shown in Fig. 10(a) (Δ^k_{SNR} = 3.0 dB) and (b) (in both cases Δ^k_{SNR} = 3.0 dB)). The corresponding restored images of Fig. 9(b) by the two choices of the regularization functional are shown in Fig. 11(a) and (b) (in both cases Δ^k_{SNR} = 4.3 dB). In all cases, the restored images by the two proposed forms of the functional $\alpha(x)$ are identical, since the values of $\alpha(x)$ at convergence are the same. The difference between the two forms of $\alpha(x)$ is demonstrated in Figs. 4 and 5. According to Fig. 4, the values of the linear $\alpha(x)$ do not converge monotonically for one of the initial conditions, although this is not the case for the quadratic $\alpha(x_k)$ for the same initial condition, as is shown in Fig. 5. In all cases, the restored images are very satisfactory, based on the improvement in SNR and visual inspection.

V. Conclusion

In this paper, we have proposed an iteration adaptive algorithm, which simultaneously determines the regularization parameter based on the restored image at each iteration step and restores the image, without any knowledge of the noise variance or the bound that is required in determining the

(a) (b)

Fig. 9. Noisy-blurred image for a 7× 7 uniform blur: (a) SNR = 20 dB; (b) (SNR = 30 dB).

(a) (b)

Fig. 10. Restored images of Fig. 9(a) by: (a) Linear choice of $\alpha(x)$; (b) quadratic choice of $\alpha(x)$.

size of the stabilizing ellipsoid in the set theoretic regularization approach. The regularization parameter now becomes a functional of the available information at each iteration and determines its value accordingly. The form and desirable properties of such a functional are analyzed in detail. It was rigorously shown in [19] that (19) also results from the hierarchical Bayesian approach if a gamma distribution is used for the hyperpriors of the hyperparameters. The resulting smoothing functional to be minimized is guaranteed to be convex, therefore, its minimizer becomes a global minimizer. This is an important improvement over our previous work on the topic [14]. An iterative algorithm is employed for obtaining the global solution. The solution now does not depend on the initial condition, as is also demonstrated experimentally. We propose overall a very useful iterative restoration algorithm that only requires knowledge of the degradation matrix D. Then, after C is determined, the algorithm operates on the available noisy-blurred image and results in an accurate restored image (based on the iterative determination of the regularization parameter), as well as in an accurate estimate of the variance of the additive noise. The analysis holds true, and the algorithm is applicable to any type of degradation D and stabilizing matrix C, in other words, there is no requirement that D and C are block circulant matrices. The incorporation of additional constraints into the restoration process, the generalized application to the multichannel images [20], and the extension of the analysis approach to the case when robust functionals are used [21] are currently under investigation.

APPENDIX A
CONDITION FOR CONVEXITY

The required conditions for convexity of $M(\alpha(x), x)$ are derived in this appendix. The left-hand side of inequality (16)

(a) (b)

Fig. 11. Restored images of Fig. 9(b) by: (a) Linear choice of $\alpha(x)$; (b) quadratic choice of $\alpha(x)$.

with the use of (14) can be rewritten as

$$M(ap_1 + (1-a)p_2, aq_1 + (1-a)q_2) = ap_1 + (1-a)p_2 + L(p_1, p_2, q_1, q_2) \quad (49)$$

where

$$L(p_1, p_2, q_1, q_2) = aq_1 f(M(ap_1 + (1-a)p_2, aq_1 + (1-a)q_2) + (1-a)q_2 f(M(ap_1 + (1-a)p_2, aq_1 + (1-a)q_2)).$$

Similarly, the right-hand side of inequality (16) can be rewritten as

$$aM(p_1, q_1) + (1-a)M(p_2, q_2) = ap_1 + (1-a)p_2 + R(p_1, p_2, q_1, q_2) \quad (50)$$

where

$$R(p_1, p_2, q_1, q_2) = aq_1 f(M(p_1, q_1)) + (1-a)q_2 f(M(p_2, q_2)).$$

Therefore, showing the validity of inequality (16) requires showing that $R(p_1, p_2, q_1, q_2) \geq L(p_1, p_2, q_1, q_2)$. For this purpose, we now use the following proposition.

Proposition 1

For $f(M)$ a linear and monotonically increasing function of M, i.e., $\frac{\partial f(M)}{\partial M} \geq 0$, it holds that

$$a_1 f(M_1) + a_2 f(M_2) \geq a_3 f(M_3) + a_4 f(M_4) \text{ if and only if } a_1 M_1 + a_2 M_2 \geq a_3 M_3 + a_4 M_4. \quad (51)$$

The proof of this proposition is shown in Appendix B.

With the use of Proposition 1, the proof of inequality (16) is simplified to showing that

$$aq_1 M[ap_1 + (1-a)p_2, aq_1 + (1-a)q_2] + (1-a)q_2 M[ap_1 + (1-a)p_2, aq_1 + (1-a)q_2] \leq aq_1 M(p_1, q_1) + (1-a)q_2 M(p_2, q_2) \quad (52)$$

based on the assumption that $f(M)$ is a linear function of M. If $M(p, q)$ were convex, then the left-hand side of inequality (52) can be bounded from above as follows

$$\begin{aligned} &aq_1 M[ap_1 + (1-a)p_2, aq_1 + (1-a)q_2] + (1-a)q_2 M[ap_1 + (1-a)p_2, aq_1 + (1-a)q_2] \\ &\quad \leq aq_1[aM(p_1, q_1) + (1-a)M(p_2, q_2)] + (1-a)q_2[aM(p_1, q_1) + (1-a)M(p_2, q_2)] \\ &\quad = a^2 q_1 M(p_1, q_1) + (1-a)^2 q_2 M(p_2, q_2) + a(1-a)[q_1 M(p_2, q_2) + q_2 M(p_1, q_1)]. \end{aligned} \quad (53)$$

We now derive the condition so that the upper bound of inequality (52) is equal to or larger than the upper bound of inequality (53). That is

$$\begin{aligned} &aq_1 M(p_1, q_1) + (1-a)q_2 M(p_2, q_2) - a^2 q_1 M(p_1, q_1) - (1-a)^2 q_2 M(p_2, q_2) - a(1-a) \\ &\quad \times [q_1 M(p_2, q_2) + q_2 M(p_1, q_1)] \\ &\quad = a(1-a)(q_1 - q_2)[M(p_1, q_1) - M(p_2, q_2)] \geq 0. \end{aligned} \quad (54)$$

Since $a(1-a)$ is always positive, the nonnegativity condition becomes

$$(q_1 - q_2)[M(p_1, q_1) - M(p_2, q_2)] \geq 0 \quad (55)$$

which is true if both terms $(q_1 - q_2)$ and $[M(p_1, q_1) - M(p_2, q_2)]$ have the same sign. Inequality (55) shows that only one of the axes q is concerned with the nonnegativity condition. It also shows that one case for $M(p, q)$ to be convex

is when $M(\cdot, q)$ is a monotonically increasing function of q, regardless of the other axis p, i.e.

$$\frac{\partial M}{\partial q} \geq 0. \tag{56}$$

Since $M = p + f(M)q$

$$\frac{\partial M}{\partial q} = \frac{\partial f}{\partial M}\frac{\partial M}{\partial q}q + f(M)$$

or

$$\frac{\partial M}{\partial q} = \frac{f(M)}{1 - q\frac{\partial f}{\partial M}} \geq 0. \tag{57}$$

Since $f(M) \geq 0$, (57) results in

$$\frac{\partial f(M)}{\partial M} < \frac{1}{q} = \frac{1}{\|Cx\|^2}. \tag{58}$$

Appendix B
Proof of Proposition 1

Since $f(\cdot)$ is a linear function, (14) can be written as

$$f(a_1M_1 + a_2M_2) \geq f(a_3M_3 + a_4M_4), \text{ iff}$$
$$a_1M_1 + a_2M_2 \geq a_3M_3 + a_4M_4. \tag{59}$$

Since $f(M)$ is a monotonically increasing function of M

$$\frac{f(M_1) - f(M_2)}{M_1 - M_2} \geq 0 \tag{60}$$

which means that both the numerator and the denominator terms should have the same sign. Therefore

$$a_1M_1 + a_2M_2 \geq a_3M_3 + a_4M_4 \tag{61}$$

is the sufficient and necessary condition for inequality (61) to hold true.

References

[1] H. C. Andrews and B. R. Hunt, *Digital Image Restoration*. Englewood Cliffs, NJ: Prentice-Hall, 1977.

[2] G. Demoment, "Image reconstruction and restoration: Overview of common estimation structures and problems," *IEEE Trans. Acoust., Speech, Signal Processing*, vol. 37, no. 12, pp. 2024–2036, Dec. 1989.

[3] A. K. Katsaggelos, Ed., *Digital Image Restoration*. Heidelberg: Springer-Verlag, Springer Series in Information Sciences, vol. 23, 1991.

[4] R. L. White and R. J. Allen, "The restoration of HST images and spectra," in *Proc. Workshop at Space Telescope Science Institute*, Baltimore, MD, Aug. 1990.

[5] A. N. Tikhonov and V. Y. Arsenin, *Solution of Ill-posed Problems*. Washington, D.C.: V. H. Winston and Sons, 1977.

[6] A. K. Katsaggelos, "Iterative image restoration algorithm," *Opt. Eng.*, vol. 28, no. 7, pp. 735–748, July 1989.

[7] A. K. Katsaggelos, J. Biemond, R. W. Schafer, and R. M. Mersereau, "A regularized iterative image restoration algorithm," *IEEE Trans. Signal Processing*, vol. 39, pp. 914–929, Apr. 1991.

[8] K. Miller, "Least-squares method for ill-posed problems with a prescribed bound," *SIAM J. Math. Anal.*, vol. 1, pp. 52–74, Feb. 1970.

[9] B. R. Hunt, "Application of constrained least squares estimation to image restoration by digital computers," *IEEE Trans. Comput.*, vol. C-22, pp. 805–812, 1973.

[10] G. Wahba, *Spline Models for Observational Data. SIAM-59*, Philadelphia, PA, 1990.

[11] S. J. Reeves and R. M. Mersereau, "Optimal estimation of the regularization parameters and stabilizing functional for regularized image restoration," *Opt. Eng.*, vol. 29, pp. 446–454, May 1990.

[12] N. P. Galatsanos and A. K. Katsaggelos, "Methods for choosing the regularization parameter and estimating the noise variance in image restoration and their relation," *IEEE Trans. Image Processing*, vol. 1, pp. 332–336, July 1992.

[13] M. G. Kang and A. K. Katsaggelos, "Simultaneous iterative image restoration and evaluation of the regularization parameter," *IEEE Trans. Signal Processing*, vol. 40, pp. 2329–2334, Sept. 1992.

[14] A. K. Katsaggelos and M. G. Kang, "Iterative evaluation of the regularization parameter in regularized image restoration," *J. Vis. Comm. Image Rep.*, vol. 3, no. 6, pp. 446–455, Dec. 1992.

[15] M. G. Kang and A. K. Katsaggelos, "Frequency domain adaptive iterative image restoration and evaluation of the regularization parameter," *Opt. Eng.*, vol. 33, no. 10, pp. 3222–3232, Oct. 1994.

[16] ——, "Regularized iterative image restoration based on an iteratively updated convex smoothing functional," in *Proc. Vis. Commun. Image Processing Conf.*, Cambridge, MA, Nov. 1993, pp. 1364–1375.

[17] F. C. Schweppe, *Uncertain Dynamic Systems*. Englewood Cliffs, NJ: Prentice-Hall, 1973.

[18] D. A. Luenberger, *Optimization by Vector Space Methods*. New York: Wiley, 1969.

[19] R. Molina and A. Katsaggelos, "The hierarchichal approach to image restoration and the iterative evaluation of the regularization parameter," in *Proc. 1994 SPIE Conf. Vis. Commun. Image Processing*, Chicago, IL, Nov. 1994, pp. 244–251.

[20] M. G. Kang and A. K. Katsaggelos, "Multichannel convex smoothing functional for simultaneous multichannel image restoration and estimation of adaptive regularization functionals," in *Proc. 1994 SPIE Conf. Vis. Commun. Image Processing*, Chicago, IL, Nov. 1994, pp. 232–243.

[21] M. E. Zervakis and T. Kwon, "Robust estimation techniques in regularized image restoration," *Opt. Eng.*, vol. 31, no. 10, pp. 2174–2190, Oct. 1992.

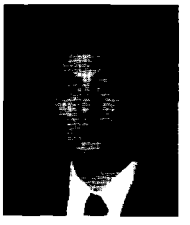

Moon Gi Kang was born in Seoul, Korea, in 1963. He received the B.S. and M.S. degrees in electronics engineering from Seoul National University, Korea, in 1986 and 1988, respectively. He received the Ph.D. degree in electrical engineering from Northwestern University in 1994.

He was a Research Assistant from 1989 to 1993 and a Research Fellow in 1994 in the Department of Electrical Engineering and Computer Science at Northwestern University. He is currently an Assistant Professor in the Department of Electrical and Computer Engineering at the University of Minnesoata, Duluth. His current research interests include regularized iterative image restoration and use of higher order spectra for image restoration.

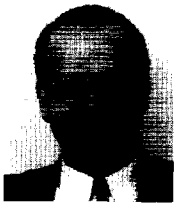

Aggelos K. Katsaggelos (S'80–M'85–SM'92) received the Diploma degree in electrical and mechanical engineering from the Aristotelian University of Thessaloniki, Thessaloniki, Greece, in 1979 and the M.S. and Ph.D. degrees in electrical engineering from the Georgia Institute of Technology, Atlanta, in 1981 and 1985, respectively.

In 1985, he joined the Department of Electrical Engineering and Computer Science at Northwestern University, Evanston, IL, where he is currently an Associate Professor. During the 1986–1987 academic year, he was an Assistant Professor at Polytechnic University, Department of Electrical Engineering and Computer Science, Brooklyn, NY. His current research interests include image recovery, processing of moving images (motion estimation, enhancement, very low bit rate compression), and computational vision.

Dr. Katsaggelos is an Ameritech Fellow and a member of the Associate Staff, Department of Medicine, at Evanston Hospital. He is a member of SPIE, the Steering Committees of the IEEE TRANSACTIONS ON MEDICAL IMAGING and the IEEE TRANSACTIONS ON IMAGE PROCESSING, the IEEE Technical Committees on Visual Signal Processing and Communications and on Image and Multi-Dimensional Signal Processing, the Technical Chamber of Commerce of Greece, and Sigma Xi. He served as an Associate Editor for the IEEE TRANSACTIONS ON SIGNAL PROCESSING (1990–1992) and is currently an Area Editor for the journal *Graphical Models and Image Processing*. He is the editor of *Digital Image Restoration* (Springer-Verlag, Heidelberg, 1991) and the General Chairman of the 1994 Visual Communications and Image Processing Conference (Chicago, IL).